DFW Microburst Model Based on AA-539 Data

Walter J. Grantham* and Guy G. Roetcisoender†
Washington State University, Pullman, Washington 99164
and
Edwin K. Parks‡
University of Arizona, Tucson, Arizona 85721

Analysis of the August 2, 1985 crash for an L-1011 jumbo jet (DL-191) on approach to the Dallas-Ft. Worth International Airport (DFW) in a thunderstorm indicates that the severe windshear microburst that caused the crash was composed not only of a strong downflow and outflow but also included several large-scale vortex rings entrained in the flowfield. This paper presents a detailed two-dimensional model of the DFW microburst based on data from the MD-80 (AA-539) that followed behind DL-191 and flew through the microburst about two minutes after the crash of DL-191. The model was developed using wind-vector and flight-path data reconstructed by NASA Ames Research Center and a combination of interactive graphics and least-squares error best fit between the modeled and measured wind vectors along the AA-539 flight path. The model indicates that the flowfield contains some significant elements and vortices not previously reported. The alternating direction of rotation of the vortices in the model suggests a microburst structure based on a von Kármán vortex street rather than on a Kelvin-Helmholtz instability. The model also indicates that the reconstructed wind-vector data contain a time lag of at least one second in the horizontal winds.

Nomenclature

a_i = horizontal offset of vortices in quadruple i from the flow centerline, m
b_i = altitude of vortex pair i above ground, m
K = rainfall centerline speed, m/s
k = index for wind-vector data (at 1/4-s intervals)
N = total number of vortex quadruples in flowfield model
n = total number of wind-vector data points
R_i = core radius of vortices in quadruple i, m
r = radial distance from vortex center, m
RMS = root-mean-square velocity error, m/s
u = horizontal component of flowfield velocity, m/s, positive to north
V_H = horizontal uniform tailwind, m/s
V_i = tangential speed at the core edge of the upper-left vortex in quadruple i, positive clockwise, m/s
v = vertical component of flowfield velocity, m/s, positive up
v_r = radial component of flowfield velocity induced by a vortex, m/s
v_θ = tangential component of induced vortex velocity, positive clockwise, m/s
x = horizontal distance north of runway, m
y = altitude above ground, m
β = rainfall exponential decay slope, 1/m
δ = horizontal wind time delay index shift (for δ/4-s time lag)
ψ = stream function, m^2/s
θ = angle (in the x-y plane) clockwise from the positive x axis, rad

Subscripts

c = centerline
i = index for vortex quadruples (pair plus mirror image)
ij = vortex j in quadruple i
j = index for vortices in a quadruple
H = horizontal wind uniform flow
R = rainfall

Superscripts

= measured (reconstructed) data

Introduction

ON August 2, 1985, an L-1011 (DL-191) crashed on final approach to the Dallas-Ft. Worth International Airport (DFW) as a result of a severe windshear microburst caused by a thunderstorm near the north end of the runway.[1] A similar crash, involving a B-727 on final approach, occurred in 1975 at New York's John F. Kennedy International Airport (JFK). Microbursts were also involved in crashes of commercial aircraft during takeoff at Denver's Stapleton Airport in 1975 and at the New Orleans airport in 1982. Over the past 20 years nearly 30 aircraft accidents have been attributed to windshear.[2] The safety hazard associated with windshear and microbursts has led to a major research effort to learn the causes and effects of severe weather phenomena.

A microburst is a strong downdraft caused by a thunderstorm, which induces strong vertical and horizontal winds called windshear.[1] It is believed that the severe wind gradients in a microburst produce a rain-driven instability between adjacent columns in the atmosphere that roll up to form vortices. The vortices are somewhat analogous to the Kelvin-Helmholtz "cat's eye" vortex patterns observed in high-altitude clear-air turbulence caused by the jet stream.[3,4] However, the results of this paper indicate that the vortex pattern may be more similar to von Kármán vortex streets, in which a sequence of vortices rotate in opposite directions rather than all in the same direction as in the case of "cats eye" vortices.

The purpose of this paper is to present a detailed two-dimensional model of the DFW microburst based on data from AA-539.[5,6] The primary purpose of this model is to determine the nature of the DFW microburst flowfield, at

Received April 1, 1989; revision received March 24, 1990; accepted for publication March 26, 1990.

*Associate Professor, Department of Mechanical and Materials Engineering. Member AIAA.
†Department of Mechanical and Materials Engineering.
‡Department of Aerospace and Mechanical Engineering. Associate Fellow AIAA.

least in the neighborhood of the AA-539 flight path. However, as a two-dimensional model, the results of this paper could be used for simulation and control studies. The results in this paper could also be used, in conjunction with an independent model based on DL-191 data,[7] to develop a time-varying model of the DFW microburst.

The results of this paper agree qualitatively with a previously published three-dimensional model[8] but include a more detailed model of the flowfield vortices as well as flowfield elements not previously modeled. In addition, the results of this paper indicate that the AA-539 wind-vector data for the DFW microburst contain at least a 1-s time lag in the horizontal wind data.

DFW Microburst Data

The L-1011 that crashed at DFW was equipped with a digital flight data recorder, providing good data on the microburst flowfield along the flight path of the aircraft. Following immediately behind DL-191, an MD-80 (AA-539), executed a go-around 110 s after the crash of DL-191 and flew through the microburst at an altitude of about 850 m. This second aircraft was also equipped with a digital flight data recorder. Based on the digital flight data records and ground-based radar data, researchers at NASA Ames Research Center have reconstructed the flight paths and wind vectors for each of the two aircraft.[5,6]

The flight path and wind vectors for both aircraft are shown in Fig. 1. In this figure, the magnitudes and directions of the reconstructed wind vectors are shown in true geometric scale even though the horizontal and vertical scales for the flight paths are different. Figures 2 and 3 show the reconstructed vertical and horizontal winds, respectively, along the AA-539 flight path. The data correspond to a 90-s period with data reconstructed at 0.25-s intervals.

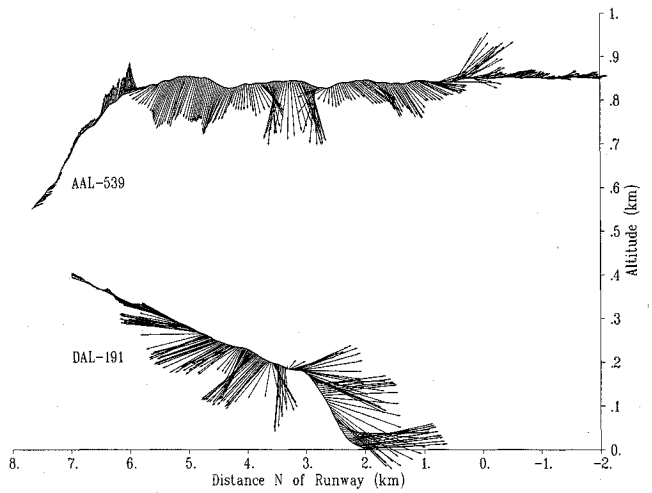

Fig. 1 Aircraft flight paths and wind vectors for the DFW microburst.

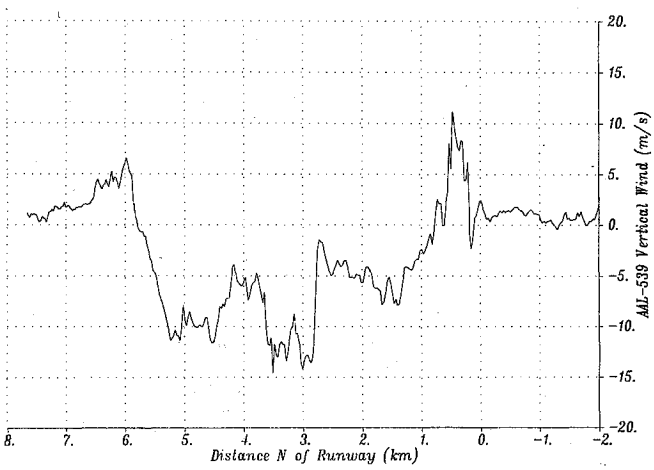

Fig. 2 AA-539 vertical wind, m/s.

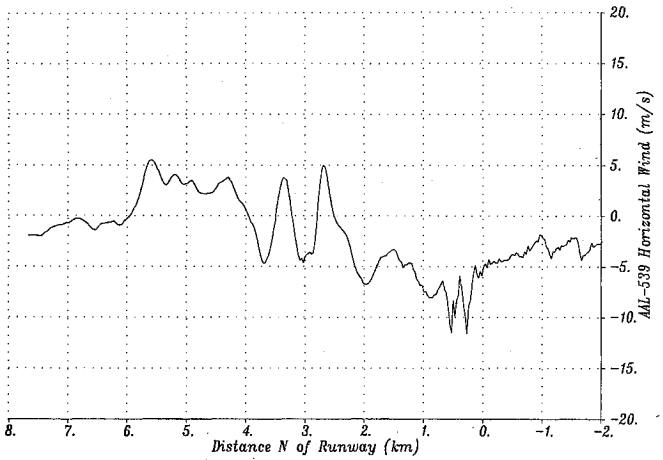

Fig. 3 AA-539 horizontal wind, m/s.

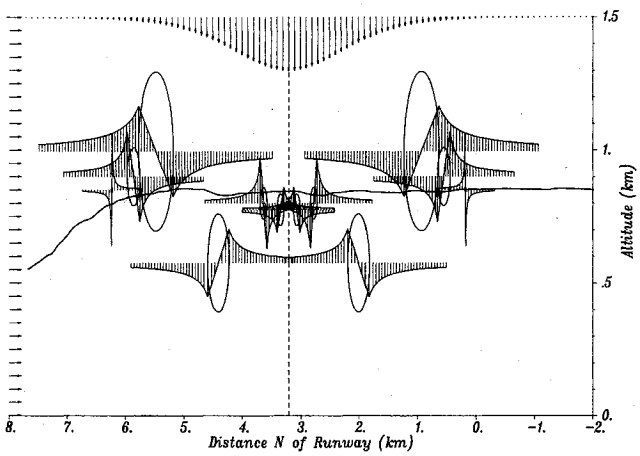

Fig. 4 DFW microburst model elements.

The model presented in this paper treats the AA-539 data as static, corresponding to an instantaneous picture of the flowfield, even though the data span a 90-s time period approximately 2 min after the crash of DL-191.

The DL-191 winds are not included in the model because of the 2-min separation between the data for the two aircraft. During the time interval the thunderstorm moved horizontally[1] and, more importantly, the vortices moved both horizontally and vertically. A subsequent paper presents a model based on DL-191 data.[7]

Microburst Model Elements

This paper presents a two-dimensional multiple vortex model of the DFW microburst flowfield based on the reconstructed flight path and the horizontal and vertical winds seen by AA-539 along its flight path.

As illustrated in Fig. 4, the elements in the model consist of six counter-rotating vortex pairs analogous to cross sections of three-dimensional vortex rings (with mirror images below the ground), an exponential rainfall distribution (with no mirror image), and a horizontal tailwind associated with lateral north-to-south motion of the thunderstorm.

To ensure that the continuity equation of fluid dynamics (conservation of mass) is satisfied, the velocity distributions for each element in the microburst model will be specified in terms of stream functions.

Because of the symmetry of the data in Figs. 2 and 3, the vortices are modeled as pairs of counter-rotating "solid-core" vortices, analogous to a cross section of a vortex ring, located symmetrically about a vertical centerline as illustrated in Fig. 5. In addition, each vortex pair has a mirror image below the ground so that the ground is a streamline for the flow associated with the vortices. Thus, each vortex "pair" actually corresponds to four vortices. The vortices are termed solid-core because they each contain a rotational core region that rotates like a rigid body. However, the term solid is a misnomer; the actual velocity at a point in vortex core is the vector sum of velocities induced by the vortex and by other flowfield elements outside of the vortex core.

Each vortex induces a flow that is rotational inside a core radius (corresponding to a "rigid-body" rotation) and irrotational outside of the core. Each vortex, by itself, has circular streamlines and induces a tangential velocity parallel to the streamlines. The collection of vortex pairs and their mirror images satisfies conservation of mass.

As illustrated in Fig. 5, the position, size, and strength of the four vortices that comprise a quadruple i (consisting of a counter-rotating vortex pair with mirror images below ground) can be specified in terms of the centerline location x_c north of the runway and four parameters.

The four vortices $j = 1,...,4$ in quadruple i have centers located at $(x,y) = (x_c + a_{ij}, b_{ij})$ and have clockwise velocities V_{ij} at their core edges, where $a_{ij} = a_i\,(-a_i)$ for vortices left (right) of the centerline, $b_{ij} = b_i\,(-b_i)$ for vortices above (below) the ground, and $V_{ij} = V_i\,(-V_i)$ for upper-left and lower-right (upper-right and lower-left) vortices.

The radial and tangential velocity components $(v_r, v_\theta)_{ij}$ induced at a point (x,y) by a vortex j in quadruple i (such as the upper-left vortex) are modeled by

$$v_{r_{ij}} = 0 \tag{1a}$$

$$v_{\theta_{ij}} = \begin{cases} V_{ij} r_{ij}/R_i & 0 \le r_{ij} \le R_i \\ V_{ij} R_i / r_{ij} & r_{ij} \ge R_i \end{cases} \tag{1b}$$

where

$$r_{ij} = \sqrt{(x - x_c - a_{ij})^2 + (y - b_{ij})^2} \tag{2}$$

is the radius from the vortex center, and

$$\theta_{ij} = \tan^{-1}\left\{\frac{y - b_{ij}}{x - x_c - a_{ij}}\right\} \tag{3}$$

is the angle of the radial vector from the vortex center to the point (x,y) measured clockwise from the positive x direction.

The flow given by Eqs. (1–3) satisfies continuity since

$$v_{r_{ij}} = \frac{1}{r_{ij}} \frac{\partial \psi_{ij}}{\partial \theta_{ij}} \tag{4a}$$

$$v_{\theta_{ij}} = -\frac{\partial \psi_{ij}}{\partial r_{ij}} \tag{4b}$$

where the stream function is

$$\psi_{ij} = \begin{cases} -(V_{ij}/2R_i) r_{ij}^2 & 0 \le r_{ij} \le R_i \\ -V_{ij} R_i \ell n r_{ij} & r_{ij} \ge R_i \end{cases} \tag{5}$$

The data for AA-539 and DL-191 indicate that the DFW microburst was moving to the south.[16] Thus, in addition to the vortices, we also model a uniform horizontal tailwind as

$$u_H = -V_H \tag{6a}$$

$$v_H = 0 \tag{6b}$$

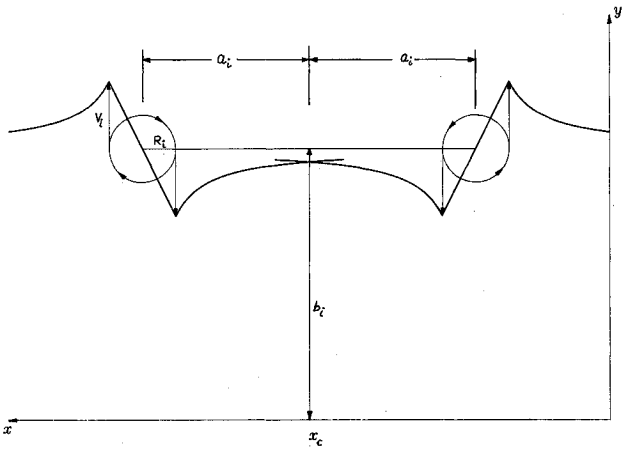

Fig. 5 Coordinate system for a vortex pair.

or, in the stream function form,

$$u_H = \frac{\partial \psi_H}{\partial y} \tag{7a}$$

$$v_H = -\frac{\partial \psi_H}{\partial x} \tag{7b}$$

where

$$\psi_H = -V_H y \tag{8}$$

Rainfall is modeled as

$$u_R = \frac{\partial \psi_R}{\partial y} \tag{9a}$$

$$v_R = -\frac{\partial \psi_R}{\partial x} \tag{9b}$$

where

$$\psi_R = (K/B)\tanh[\beta(x - x_c)] \tag{10}$$

is the stream function for a vertical rainfall independent of altitude but exponentially decaying with distance from the vortex ensemble centerline. Note that we do not employ a mirror image of the rainfall below the ground; to do so would simply cancel the rainfall.

It should also be noted that the rainfall distribution, like the vortex cores, is rotational. In the absence of the rainfall, the flowfield outside of the vortex cores would be irrotational. With the rainfall, which acts throughout the flowfield, the entire flowfield is rotational.

The model outlined in this section satisfies the equation of continuity for incompressible fluids, since the overall flowfield is derivable from a stream function constructed by converting to a common (x,y) coordinate system and summing all of the component stream functions. The resulting stream function is given by

$$\psi(x,y) = \psi_R(x,y) + \psi_H(x,y) + \sum_{i=1}^{N} \sum_{j=1}^{4} \psi_{ij}(x,y) \tag{11}$$

However, because of the rainfall, the ground is not a streamline. Considered as a two-phase flow of air and rain, the ground is a streamline for the airflow, but the mass flow rate of the rainfall is absorbed by the ground.

Parameter Identification

As demonstrated in Ref. 4, an initial estimate for the location of vortices can be developed by a graphical examina-

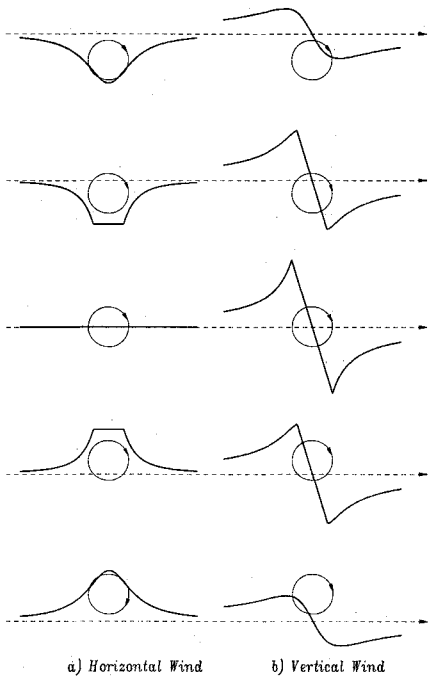

Fig. 6 Horizontal and vertical winds for flight past a vortex.

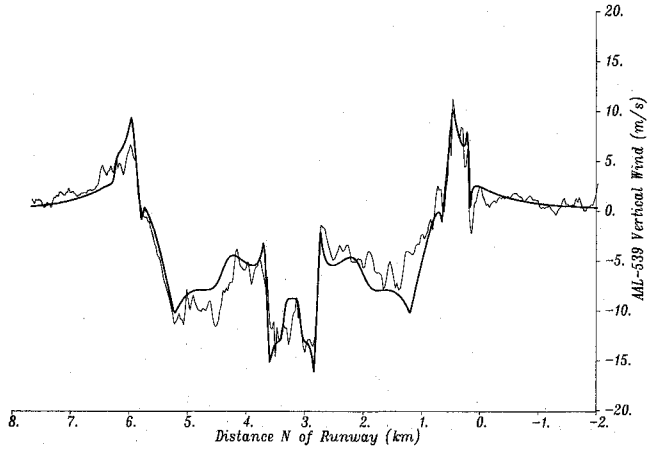

Fig. 7 AA-539 vertical wind for the model (thick) and data (thin).

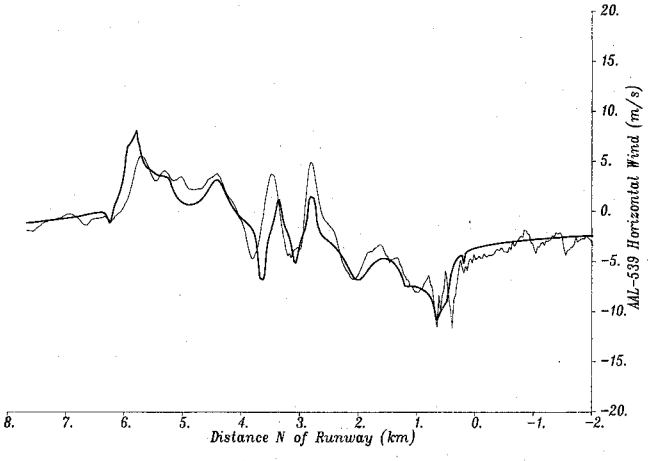

Fig. 8 AA-539 horizontal wind for the model (thick) and time-delayed data (thin).

Table 1 DFW microburst vortex-pair parameter values

Parameter	Vortex pair					
	1	2	3	4	5	6
Core radius R_i, m	60	60	185	300	110	10
Horizontal offset a_i, m	140	430	1200	2275	2655	3025
Altitude b_i, m	775	800	575	995	900	850
Edge velocity V_i, m/s	−4.0	8.0	−6.0	8.0	8.0	−10.0

Table 2 DFW microburst model parameter values

Parameter	Value
Centerline location x_c, m	3215
Rainfall centerline speed K, m/s	9.5
Rainfall exponential decay β, 1/m	7.7×10^{-4}
Horizontal uniform tailwind V_H, m/s	2.0
Horiz. wind data time lag $\delta/4$, s	1.00
RMS velocity error, m/s	
Vertical wind	1.709
Horizontal wind	1.664
Total	2.385

tion of the peaks and valleys in the vertical and horizontal wind data.

As illustrated in Fig. 6, when an aircraft flies past a vortex core, a minimum or maximum will occur in the horizontal wind at a point corresponding to the center of the vortex. For a clockwise vortex rotation and an aircraft flying from left to right and above (below) the core, a minimum (maximum) will occur in the horizontal location of the vortex center is crossed. In addition, an essentially straight-line maximum-to-minimum transition will occur in the vertical wind as the aircraft flies past the vortex core, either above or below. Vertical wind maximum and minimum points correspond to the edges of the vortex core and the midpoint corresponds to the horizontal location of the vortex center. For a counterclockwise vortex rotation, "maximum" and "minimum" interchange in this discussion.

It should be noted that horizontal and vertical wind maxima and minima provide two independent estimates of the horizontal location of vortex cores. As we shall see, the data yield a discrepancy between these two estimates. We will use the estimates based on the vertical wind data and will synchronize the horizontal wind data by introducing a horizontal wind time lag (of approximately 1 s), which slides the horizontal wind plot slightly to the left in Fig. 3. This time lag, which occurs to an even greater degree in the DL-191 data, may be attributed to errors in the aircraft's pitot-static system for measuring dynamic pressure, which is used to reconstruct the horizontal winds. These errors are caused in part by the relatively slow response of pitot-static systems (which can be modeled as a first-order dynamical system) in a rapidly changing environment compared to the response time of accelerometers or angle-of-attack measurement systems used to reconstruct vertical winds. This lag error may also be due to angle-of-attack orientation errors in the pitot-static system[9] caused by strong vertical wind gradients.

The parameters determined graphically for an initial flowfield model were further tuned to minimize the RMS error between the measured and modeled vertical and horizontal

winds along the 90-s AA-539 flight path segment shown in Fig. 1. Let k index the measured wind data (at 0.25-s intervals). Let $u'(k)$ and $v'(k)$ be the measured (reconstructed) horizontal and vertical winds, respectively, at time index k, and let $u(k)$ and $v(k)$ be the modeled horizontal and vertical winds at the corresponding point in the flowfield.

The RMS error is given by

$$\text{RMS} = \left\{\frac{1}{n}\sum_{k=1}^{n}([u(k) - u'(k-\delta)]^2 + [v(k) - v'(k)]^2)\right\}^{1/2} \quad (12)$$

where n is the number of data points and δ is an index shift factor to allow for the possibility of a horizontal wind time lag of $\delta/4$ s.

The RMS error turns out to be a less than ideal performance measure. When applied for optimization of all parameters in the model, the minimum RMS criterion tended to yield a model with the peaks and valleys smoothed out. Since the uncertain wind gradients have a signficant effect on the control of aircraft in a microburst,[10] some criterion which detects peaks, valleys, and slopes in the data might have been better.

The approach that we employed involved using graphic estimates for the horizontal centerline location and for the radius and horizontal offset of counter-rotating vortex pairs. Optimization of the RMS error was used to selectively determine the altitude and tangential velocity for individual vortex pairs and to determine the parameters for a rainfall model and for a uniform horizontal tailwind corresponding to motion of the thunderstorm.

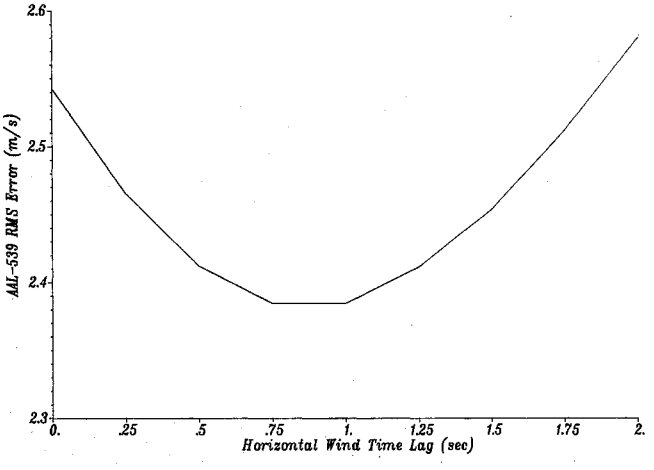

Fig. 9 The effect of a horizontal wind data time lag of $\delta/4$ s.

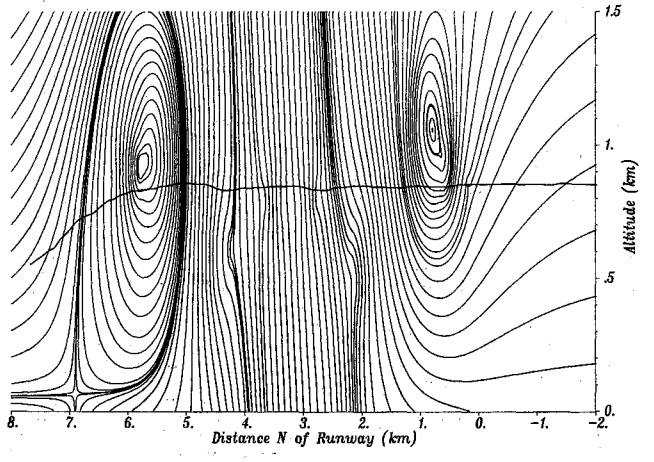

Fig. 10 Streamlines for the DFW microburst model flowfield.

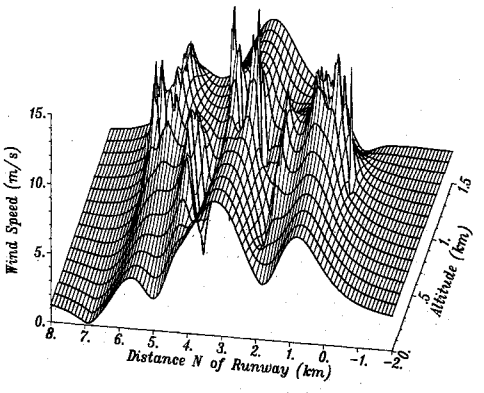

Fig. 11 Wind speed in the vertical plane of the DFW microburst flowfield.

DFW Microburst Model

Tables 1 and 2 show the parameter values and the RMS error for the DFW microburst model presented in this paper. Figures 7 and 8 show a comparison of the measured and modeled vertical and horizontal winds, with the measured horizontal wind having been shifted slightly to the left in Fig. 8 compared to Fig. 3. Figure 9 shows the effect on the RMS value of varying the horizontal wind time lag. Figure 10 shows the streamlines for the flowfield model, and Fig. 11 shows a three-dimensional plot of the wind speed throughout the region shown in Fig. 10.

The accuracy of the model is illustrated by the agreement between measured and modeled winds evident in Figs. 7 and 8. The RMS error (2.385 m/s) for this model is very low and is evenly distributed between the vertical and horizontal winds, which have RMS errors by themselves of 1.709 m/s and 1.664 m/s, respectively, with the overall RMS error being the square root of the sum of the squares of these two individual values. To put the overall RMS error in some perspective, the RMS error of the data itself against a still-air model (with no horizontal wind data time lag) is 7.120 m/s, distributed 60% in the vertical wind data and 40% in the horizontal wind data.

The 1-s horizontal wind data time lag incorporated in the model results in a shift of the data approximately 109 m to the left in Fig. 8, corresponding to an AA-539 ground speed of 109 m/s. This 1-s lag is a compromise. For the major features at the far left and right in Fig. 8, a better qualitative and quantitative fit would result from using a 3-s horizontal wind time lag. This value, which would also be consistent with a first-order dynamical system model of a pitot-static system, would, however, result in a poorer fit near the centerline of the flowfield.

Conclusions

The DFW microburst model presented in this paper agrees very well with measured data, provided a slight time delay is assumed in the horizontal wind data. The results clearly indicate the presence and effect of such a time lag. In addition, the model presented in this paper is more detailed than the previous result[8] and indicates that the large vortex ring reported in Ref. 8 is actually two vortex rings (vortex pairs 4 and 5 in Table 1) whose cores meet tangentially, as illustrated in Fig. 4. The model also reveals an interesting pattern of vortices, in which the vortices (except for the single ring in Ref. 8, which became two vortex pairs in Table 1) alternate in their direction of rotation outward from the flowfield centerline instead of the case of the two vortex rings reported in Ref. 8, which both rotated in the same direction. This result suggests that the vortex pattern may be more analogous to von Kármán vortex streets than to the Kelvin-Helmholtz cat's eye vortices associated with high-altitude clear-air turbulence.[3,4]

The results of this paper show that the flowfield contained some strong low-altitude vortices, whose large vertical wind gradients occurred at about the same place where DL-191 had a sudden, final loss of altitude. This result, along with the aircraft control results in Ref. 10, suggests that strong vertical wind gradients may be one of the dangerous aspects of a microburst, in addition to a well-known headwind-to-tailwind shift.

The flowfield model presented in this paper is based solely on the data for AA-539. Experience in the development of the model suggests that the model is only valid near the AA-539 flight path, since vortices away from the flight path decay rapidly and may not be evident from the AA-539 data. In particular, a model based on DL-191 data may show vortices not sensed by the AA-539 data. Alternatively, a DL-191-based model may show the same major vortices as seen by AA-539, but in different positions because of the 2-min separation between the two flights. A subsequent paper[7] will present a DL-191-based DFW microburst model for comparison.

Acknowledgment

Funds for the support of this study have been allocated by NASA Ames Research Center, Moffett Field, CA, under Interchange NCA 2-216 and Contract NCC 2-329.

References

[1]Fujita, T. T., *DFW Microburst*, Univ. of Chicago, Chicago, IL, Satellite and Mesometeorology Research Project, SMRP 217, 1986.

[2]Miele, A., Wang, H., Wang, T., and Melvin, W. W., "Optimal Penetration Landing Trajectories in the Presence of Windshear," *Journal of Optimization Theory and Applications*, Vol. 57, No. 1, April 1988, pp. 1–40.

[3]Parks, E. K., Wingrove, R. C., Bach, R. E., and Mehta, R. S., "Identification of Vortex-Induced Clear Air Turbulence Using Airline Flight Records," *Journal of Aircraft*, Vol. 22, No. 2, 1985, pp. 124–129.

[4]Mehta, R. S., "Modelling Clear-Air Turbulence with Vortices using Parameter-Identification Techniques," *Journal of Guidance, Control, and Dynamics*, Vol. 10, No. 1, 1987, pp. 27–31.

[5]Bach, R. E., Jr., and Wingrove, R. C., "The Analysis of Airline Flight Records for Winds and Performance with Application to the Delta 191 Accident," *Proceedings of the AIAA Atmospheric Flight Mechanics Conference*, AIAA, New York, 1986, pp. 361–373.

[6]Wingrove, R. C., and Bach, R. E., Jr., "Severe Winds in the DFW Microburst Measured from Two Aircraft," *Proceedings of the AIAA Guidance, Navigation, and Control Conference*, AIAA, Washington, DC, 1987, pp. 477–482.

[7]Grantham, W. J., and Parks, E. K., "A DFW Microburst Model Based on DL-191 Data," *Proceedings of the 29th IEEE Conference on Decision and Control*, W.P.-VIII-1-3, Institute of Electrical and Electronic Engineers, New York (to be published).

[8]Schultz, T. A., "A Multiple-Vortex-Ring Model of the DFW Microburst," AIAA Paper 88-0685, 1988.

[9]Sabersky, R. H., and Acosta, A. J., *Fluid Flow*, Macmillan, New York, 1964.

[10]Leitmann, G., and Pandey, S., "Aircraft Control under Conditions of Windshear," *Advances in Control and Dynamic Systems*, Vol. 34, edited by C. T. Leondes, Academic, San Diego, CA, 1990, pp. 1–79.